# Comparative analysis of gene expression profiles in differentiated subcutaneous adipocytes between Jiaxing Black and Large White Pigs

**Dawei Zhang**
Jiaxing University https://orcid.org/0000-0002-7894-7603
**Wenjing Wu**
Jiaxing University
**Xin Huang**
Hebei Normal University of Science and Technology
**Ke Xu**
Hebei Normal University of Science and Technology
**Cheng Zheng**
Hebei Normal University of Science and Technology
**Jin Zhang** ( zhangjin7688@163.com )
Jiaxing University

**Research article**

**Keywords:** Subcutaneous fat, Pig, Sus scrofa, LncRNA, mRNA, RNA-seq

**Posted Date:** April 9th, 2020

**DOI:** https://doi.org/10.21203/rs.3.rs-19837/v1



**Version of Record:** A version of this preprint was published on January 19th, 2021. See the published version at https://doi.org/10.1186/s12864-020-07361-9.

# Abstract

Background: Chinese domestic pig breeds are reputed for pork quality, but their low ratio of lean-to-fat carcass weight decreases production efficiency. A better understanding of the genetic regulation network of SC fat tissue is necessary for the rational selection of Chinese domestic pig breeds. In the present study, SC adipocytes were isolated from Jiaxing Black pigs (a Chinese indigenous pig breed with redundant SC fat deposition) and Large White pigs (a lean-type pig breed with relatively low SC fat deposition) and the expression profiles of mRNAs and lncRNAs were compared by RNA-seq analysis to identify biomarkers correlated with the differences of SC fat deposition between the two breeds.

Results: A total of 3,371 differentially expressed genes (DEGs) and 1,182 differentially expressed lncRNAs (DELs) were identified in SC adipocytes between Jiaxing Black (JX) and Large White (LW) pigs, which included 797 upregulated mRNAs, 2,574 downregulated mRNAs, 461 upregulated lncRNAs and 721 downregulated lncRNAs. Gene Ontology and KEGG pathway analyses revealed that the DEGs and DELs were mainly involved in the immune response, cell fate determination, PI3K-Akt signaling pathway and MAPK signaling pathway, which are known to be related to adipogenesis and lipid metabolism. The expression levels of DEGs and DELs according to the RNA-seq data were verified by quantitative PCR, which showed 81.8% consistency. The differences in MAPK pathway activity between JX and LW pigs was confirmed by western blot analysis, with <100-fold elevated p38 phosphorylation in JX pigs.

Conclusions: This study offers a detailed characterization of mRNAs and lncRNAs in fat- and lean-type pig breeds. The activity of the MAPK signaling pathway was found to be associated with subcutaneous adipogenesis. These results greatly enhance our understanding of the molecular mechanisms regulating SC fat deposition in pigs.


# Background

Fat deposition is one of the most important economic traits of pigs. The size of subcutaneous (SC) fat deposits is associated with lean meat carcass percentage, while intramuscular (IM) fat content is the main factor affecting pork quality[1]. Foreign pig breeds, such as Duroc, Large white, and Landrace, deposit low level of SC fat, while Chinese indigenous pig breeds, such as Laiwu, Taihu, and Jinhua, deposit high levels of SC fat[2–6]. Excessive SC fat deposition greatly decreases the growth performance and meat production efficiency, which results in profit reduction[7, 8]. However, Chinese indigenous pig breeds often exhibit better fertility, disease resistance and IM fat content than foreign pig breeds[9–11]. Understanding the porcine adipocyte regulation network to decrease SC fat deposition is a key issue in genetic improvement of Chinese indigenous pig breeds. In addition, human health problems caused by excessive fat accumulation are becoming increasingly common. It has been demonstrated that obesity increases the risk for the development of type 2 diabetes mellitus, cardiovascular disease, hypertension, dyslipidemia, and certain types of cancer[12, 13]. Notably, pigs can be used in biomedical studies due to their anatomic and physiological similarity to humans[14, 15]. Therefore, clarifying the molecular

mechanisms of SC fat deposition in pigs can not only benefit the genetic breeding of pigs, but also deepen the understanding of human metabolic diseases.

Porcine SC fat deposition is largely determined by the proliferation and differentiation of adipocytes[16]. With the advent of omics technologies, many genes and pathways regulating the metabolism of porcine adipocytes have been identified[17–19]. Recently, the regulatory role of long noncoding RNAs (lncRNAs) in porcine adipogenesis has been reported by several groups[20, 21]. LncRNAs are defined as a class of transcribed RNA molecules that are more than 200 nucleotides in length and do not encode proteins[22]. LncRNAs can interact with DNA, RNA or proteins, and regulate gene expression via diverse mechanisms. It has been estimated that lncRNAs with a well-described functional role constitute less than 1% of the lncRNAs in organisms[23]. Thus, identifying the regulatory role of lncRNAs in porcine adipogenesis is of great importance for understanding the molecular mechanisms that regulate SC fat deposition in pigs.

Jiaxing Black pig (JX pig), a Chinese indigenous pig breed in the Taihu Lake region, is famous for its early sexual maturity, high fecundity, crude feed tolerance, good hybridization ability and plump muscles with a high content of IM fat. Products derived from JX pigs have been developed into a well-recognized commercial pork brand in China[24]. However, the redundant SC fat deposition decreases the growth efficiency and results in profit reduction. By contrast, Large White pig is the most widely distributed lean-type pig breed with relatively low SC fat deposition[11]. In this study, high-throughput RNA-seq was conducted to compare the gene expression profiles of differentiated SC adipocytes from the two pig breeds. LncRNAs and genes associated with porcine adipogenesis or lipid metabolism were identified. Furthermore, functional enrichments and interaction network analyses were conducted to investigate the molecular mechanisms of differentially expressed lncRNAs and genes regulating fat deposition, which provides new knowledge for understanding the regulatory network of SC fat deposition in pigs.

## Results

# RNA-seq analysis of subcutaneous adipocytes from Jiaxing black pig and Large white pig

Primary cultures of SC adipocytes were isolated from 3-day-old Jiaxing Black (JX) and Large White (LW) pigs, and subjected eight days of differentiation. The differentiated adipocytes were harvested and subjected to RNA-seq analysis in three biological replicates. The Illumina HiSeq platform provided an average of 15.2 GB of clean reads for each sample. The percentage of clean reads among the raw data in each library ranged from 91.444–95.103%. For each sample, 90.22%, 87.20%, 86.05%, 84.79%, 85.59% and 85.76% unique reads could be mapped to the current version of the pig genome (Sscrofa 11.1), representing 23290, 22269, 22597, 22201, 21809 and 21981 genes, respectively (Supplementary Table 1). Gene numbers within a certain range of FPKM values were analyzed, and each sample gave similar results (Supplementary Fig. 1A). The distribution of log10 transformed FPKM values indicated the expression levels of transcripts. In each breed, the mRNA expression levels were relatively higher than those of lncRNAs, as expected, while both mRNAs and lncRNAs showed similar distribution in both

breeds (Supplementary Figs. 1B and 1C). Taken together, both the biological replicates and sequencing data indicated sufficiently good quality for further analysis.

# Differentially expressed lncRNAs and genes in subcutaneous adipocytes from the two breeds

To further understand the differences of SC adipocytes between the two breeds, comparative transcriptome analysis was conducted. A total of 4553 differentially expressed RNAs were identified, including 1258 up- and 3295 downregulated RNAs in SC adipocytes between the two breeds (Fig. 1A). Among these differentially expressed RNAs, 3371 were mRNAs (DEGs) and 1182 were lncRNAs (DELs). Among the 3371 DEGs, 797 were up- and 2574 were downregulated. Among the 1182 DELs, 461 were up- and 721 were downregulated (Fig. 1B). Among these differentially expressed mRNAs and lncRNAs, 2464 differentially expressed genes (DEGs) and 429 DELs had been previously annotated, and 907 DEGs and 753 DELs were novel (Fig. 1C).

# Functional enrichment analysis of differentially expressed genes

The potential functions and signaling pathways of the differentially expressed genes (DEGs) were analyzed by Gene Ontology (GO) and Kyoto Encyclopedia of Genes and Genomes (KEGG) enrichment analysis. GO analysis based on biological process was conducted and the top 20 most highly enriched categories were listed (Fig. 2A). The results showed that DEGs related to cell proliferation, differentiation, migration, adhesion, apoptosis and cell-cell signaling were significantly enriched. Four processes related to immune response, namely “response to lipopolysaccharide”, “inflammatory response”, “immune response”, and “defense response to virus”, were also detected. Two terms closely associated with lipid metabolism were also identified. These were “calcium ion binding” and “positive regulation of ERK1 and ERK2 cascade”. In addition, the enrichment based on KEGG analysis was performed and the top 20 pathways are presented in Fig. 2B. Among these results, several immune-related pathways also appeared, such as “Chemokine signaling pathway”, “Systemic lupus erythematosus”, “Tuberculosis”, “Cytokine-cytokine receptor interaction”, “Leukocyte transendothelial migration”, “Phagosome” and “Rheumatoid arthritis”. Moreover, “Ras signaling pathway”, “PI3K-Akt signaling pathway”, “Osteoclast differentiation”, and “MAPK signaling pathway” were significantly enriched, all of which are highly associated with adipocyte differentiation and lipid accumulation. The results of enrichment analysis illustrated the regulatory differences of SC fat deposition between JX and LW pigs.

# Protein-protein interaction network analysis

In unsupervised hierarchical clustering analysis, heat maps were generated using the differentially expressed DEGs, and they clearly self-segregated into different clusters for JX and LW pigs. These results reflected the distinct mRNA expression profiles of the two breeds (Fig. 3A). The protein-protein network was constructed using the top 20 DEGs ranked using the Maximal Clique Centrality (MCC) topological algorithm. As can be seen in the network shown in Fig. 3B, six DEGs were closely related to the distinctions of SC fat differentiation in both breeds. Compared to LW pigs, three DEGs (MMP9, MKI67 and VCL) were up- and three (SPTAN1, TLR2 and KIT) were downregulated in differentiated subcutaneous adipocytes of JX pigs (Fig. 3C).

# Functional enrichment analysis of lncRNAs based on target genes

Based on RNA-seq data, the potential target genes of DELs were predicted to explore their potential functions. In GO enrichment analysis, the two immunity-related terms “positive regulation of I-κB kinase/NFκB signaling” and “innate immune response”, were detected. The categories cell proliferation, apoptosis and cell adhesion, which were detected in the DGE analysis, were also identified here (Fig. 4A). In KEGG enrichment analysis, four pathways related to adipocyte differentiation and lipid accumulation were identified, including “PI3K-Akt signaling pathway”, “cGMP-PKG signaling pathway”, “MAPK signaling pathway” and “Calcium signaling pathway” (Fig. 4B). In addition, the protein-protein network was constructed to offer new insights into the related biological processes. Compared to expression levels in LW pigs, a quarter of the target genes were up- and three quarters were downregulated in JX pigs (Fig. 4C). Among the interacting genes, *Rab7a*, *WDR12*, *LPAR1*, *TBX5*, *Dicer1*, *WEE1*, *CDC25B*, *WDR12*, *CAPZB*, *UVRAG*, and *ST6Gal-I*, are known to participate in the regulation of cell proliferation or differentiation. Furthermore, *Dicer1*, *TBX5*, *TMEM173*, *PRPF8*, *AKAP9*, *ZBP1*, *UVRAG*, *ST6Gal-I*, *LRRFIP2*, and *HDAC10* are known to mediate the immune response. Moreover, *LPAR1*, *LPAR1*and *AKAP9* were also reported to be associated with the PI3K/AKT signaling pathway or MAPK signaling pathway. Significantly, *Nfe2l1*and *PLAG1* were reported to have an impact on the plasticity of adipose tissue. Thus, the DELs might play an essential role in the distinct adipogenesis of JX pigs.

# Validation of the differentially expressed genes and lncRNAs

To validate the reliability of the RNA-seq results, 12 differentially expressed genes (DEGs) and 10 lncRNAs (DELs) were randomly chosen for quantitative PCR (qPCR) verification (Fig. 5A-5D). Compared with the RNA-seq data, 10 DEGs and 8 DELs gave consistent results, while two DEGs (*MGP* and *RESTI)* and two DELs (aXR_002337668.1 and LTCONS_00084076) showed statistically different results by qPCR analysis. Overall, 81.8% of the results were in agreement between the two techniques.

# Verification of the pathway analysis

Because the MAPK signaling pathway was identified in the functional enrichment analysis of both DEGs and DELs, its activity in SC fat tissues of the two breeds was examined. Expression levels and phosphorylation of two kinases in the MAPK pathway, ERK1/2 and p38, were determined by western blot analysis. ERK1/2 showed no differences in total protein abundance or phosphorylation between the two breeds. However, while the total protein abundance of p38 was similar, the abundance of phosphorylated p38 showed a remarkably large difference between the two breeds. While p38 phosphorylation was practically absent in LW pig samples, it presented a heavy band in the JX pig samples (Fig. 6). The difference of p38 phosphorylation indicated that the activity of the MAPK pathway in SC fat tissue varied significantly between the two breeds, which confirmed the results of pathway enrichment analysis.

# Discussion

Subcutaneous (SC) fat tissue has multiple functions in pigs, including thermal insulation, energy storage and adipokine secretion[25, 26]. However, the reduction of SC fat content is of great importance for pig production because fat deposition wastes a lot of energy[7]. Therefore, excessive triglyceride accumulation in SC fat tissues is unfavorable for both energy utilization and lean meat production of pigs. Many Chinese domestic pig breeds are reputed for their high pork quality, but their low ratio of lean-to-fat carcass weight decreases production efficiency. Consequently, a better understanding of the regulation network in SC fat tissue is necessary for the rational genetic improvement of Chinese domestic pig breeds. In this study, gene expression profiles of SC adipocytes from the local Jiaxing Black (JX) pig and Large White (LW) pig were compared via RNA-seq analysis. A total of 4553 differentially expressed RNAs were identified, including 3,371 mRNAs encoded by protein-coding genes (DEGs) and 1,182 lncRNAs (DELs). These results were validated by qPCR analysis, which indicated that the data are reliable, with 81.8% consistency.

In order to identify the differences of the regulation network in SC adipocytes from the two pig breeds, GO and KEGG pathway enrichment analyses were performed. DEGs and target genes of DELs were mainly enriched in three pathways related to lipid metabolism and adipocyte differentiation, namely, “Calcium signaling pathway”, “PI3K-Akt signaling pathway” and “MAPK signaling pathway”. The calcium signaling pathway can regulate lipolysis and the accumulation of adipose tissue by changing the concentration of calcium ions in adipocytes[27, 28]. PI3Ks are a group of intracellular lipid kinases, which phosphorylate phosphatidylinositol and phosphoinositide to generate new intracellular second messengers[29]. These messengers in turn activate many intracellular signaling pathways and regulate various biological process in cells[30]. Plum et al. reported that the PI3K signaling pathway is induced by leptin and participates in biological processes related to obesity [31]. Insulin signaling via the PI3K/Akt axis plays an important role within adipocytes of obese patients, where the excess of lipids has to be properly stored in fat tissue[32]. The MAPK signaling pathway is common to several cell types, and it is involved in many biological processes, including cell proliferation, differentiation, development, and apoptosis[33]. The MAPK signaling pathway was among the top 20 most highly enriched pathways in KEGG analysis, and

the GO annotation of DEGs uncovered the ERK1, ERK2 cascade, which indicates the activity of MAPK signaling pathway [34]. Therefore, the results of this study indicate that the MAPK signaling pathway may be important for mediating subcutaneous adipogenesis in Jiaxing Black pigs. Considering that ERK and p38 are two main kinases in the MAPK pathway, and opposite results were observed for the regulatory functions of ERK and p38 during adipocyte differentiation[35–37], we further compared the activation of p38/ERK in subcutaneous adipose tissue of the two pig breeds. We found that there was practically no p38 phosphorylation in LW pigs, which contrasted with high abundance of phosphorylated p38 in JX pig adipocytes. Most studies performed in cell lines described a positive role of p38 in adipogenesis, and a decrease of C/EBPβ phosphorylation and PPARγ transactivation activity was observed when p38 activation was inhibited[35]. Moreover, mice lacking p38α in adipose tissues displayed a lean phenotype, improved metabolism, and resistance to diet-induced obesity[38]. Thus, a precise understanding of the regulatory mechanism of these two pathways will be crucial for revealing the reason why Jiaxing Black pigs have a lower lean carcass weight ratio, and will be helpful for efficiently treating obesity.

Healthy adipose tissue is minimally infiltrated by immune cells, which serve as sentinels to detect invaders[39, 40]. These cells also exert housekeeping functions that help maintain tissue integrity[41, 42]. In this study, we discovered that many immune-related signaling pathways, such as the inflammatory response, innate immune response, tuberculosis, HTLV-I infection, phagosome and cytokine-cytokine receptor interaction, were enriched in GO and KEGG enrichment analysis. Thus, the obtained differential expression profiles of mRNAs and lncRNAs indicated that there are potential functions of cytokines and immune cells in the fat deposition and metabolism of pigs. In addition to maintaining the structural integrity, these pathways can also regulate the endocrine functions of adipose tissues[43, 44]. Consequently, our results provide evidence that subcutaneous adipogenesis in pigs is related to the immune landscape of porcine adipose tissues. In addition, it should be noted that other types of proteinases are also known to be involved in adipogenesis. Some matrix metalloproteases (MMPs) are expressed in adipose tissues, secreted into the plasma, and can act as a paracrine factors. Several groups showed that MMP2 or MMP9 possess adipogenesis-enhancing activity[45]. In the predicted protein-protein interaction network from this study, MMP9 was at a key and core node. Taken together, the activity of the identified signaling pathways can explain the regulatory network of porcine SC adipocyte from each breed.

# Conclusions

In summary, a comparative transcriptome analysis of porcine SC adipocytes between Jiaxing Black and Large White pigs was conducted. A large number of differentially expressed genes and lncRNAs were identified. Elevated activity of the MAPK/p38 pathway was detected in the SC fat of Jiaxing Black pigs. Taken together, the results may help explain the excessive fat deposition of Jiaxing Black pigs and offer a clue for genetic improvement of Chinese domestic pig breeds.

## Methods

# Experimental animals

All experimental procedures involving animals were performed in accordance with the guidelines of the Animal Care and Use Committee at the Jiaxing University. The experimental animals used here included 3 male Jiaxing Black pigs and 3 male Large White pigs, which were 3-day-old and provided by Zhejiang Qinglian Food Co., Ltd (Jiaxing, Zhejiang Province, China). The piglets were raised under the same feeding and environmental conditions. All piglets were sacrificed using a $CO_2$ euthanasia box, after which the subcutaneous adipose tissues were collected for the primary culture of subcutaneous adipocytes.

# Preadipocyte culture and differentiation

Porcine subcutaneous adipose tissue isolated from male piglet was washed three times with serum-free DMEM/F12 medium. Then, tissues were aseptically cut into pieces and incubated with 1 mg/mL type I collagenase (Invitrogen, Carlsbad, CA, USA) at 37 °C for an hour. The digestion solution was filtrated through a 200 μm nylon mesh, after which the preadipocytes were collected by centrifuged at 1,000 rpm for 10 min, and cultured in DMEM/F12 medium (HyClone, USA) containing 10% fetal bovine serum (FBS; Gibco, USB) and 1% penicillin-streptomycin at 37 °C in a humidified atmosphere comprising 5% $CO_2$. After the preadipocytes reached confluence (designated as experimental day 0), the differentiation cocktail comprising DMEM/F12 supplemented with 10% FBS, 0.5 mM isobutyl methylxanthine (IBMX; Sigma, USA), 0.5 mM dexamethasone (Sigma, USA), and 20 nM insulin (Sigma, USA) was added to induce cell differentiation for 2 days, after which the cells were maintained in DMEM/F12 medium supplemented with 10% FBS and 20 nM insulin for an additional 8 days.

# RNA isolations and Illumina sequencing

Differentiated subcutaneous adipocytes from three biological replicates were subjected for RNA isolation using Trizol reagent (Invitrogen, USA). The RNA quality and concentration were measured using a NanoDrop One (Thermo Fisher Scientific, USA) and agarose gel electrophoresis. The RNA was stored at -80°C until further use. Ribosomal RNA from each sample was removed using the Ribo-Zero™ rRNA Removal Kit (Epicentre, USA), after which the purified RNA was fragmented and reversely transcribed to synthesize the first-strand cDNA using the TruSeq® First-Strand kit (Illumina, USA). The double-stranded cDNA (ds-cDNA) was synthesized in a reaction mixture comprising buffer, dNTPs, RNase H and DNA polymerase I, and the end of ds-cDNA was ligated with an ‘A’ base and sequencing linker. The entire library was completed by performing amplification of ligation products and sequenced using an Illumina 2000 platform.

# Reference genome mapping and gene quantification

After removing low-quality reads from the raw reads using SOAP, the remaining sequences were aligned to the reference genome Sscrofa 11.1 using HISAT software. The resulting alignment data were then fed into StringTie for transcriptome assembly, and Cufflinks was used to map the sequencing transcripts to reference transcripts. Subsequently, the abundance of transcripts was determined using the Fragments Per Kilobase of exon per Million fragments mapped (FPKM) method.

# LncRNA identification

The criteria for candidate lncRNAs identification were as follows: Firstly, transcripts shorter than 200nt or less than two exons were filtered out; Secondly, the tools encoding potential calculator (CPC), coding-non-coding index (CNCI), txCdsPredict and protein folding domain database (Pfam) were used for lncRNA screening. The lncRNAs that appeared as hits in at least three of the four software tools were included in the final result. To identify the known lncRNAs, lncRNA candidates were aligned to the ALDB database (A Domestic Animal Long Noncoding RNA Database) with the following settings: identity (100%), mismatch (0), E-value (<1e-10) and gap opening (0).

# Differential expression analysis

The FPKM value and DEGseq algorithm were used to determine expression levels of genes and lncRNAs. Genes and lncRNAs with padj (adjusted P value) $\leq 0.05$ were considered to be differentially expressed.

# LncRNA target gene prediction

LncRNAs can function by two different modes, either as cis-regulators of neighboring target genes or as trans-regulators distant target genes. For cis-acting lncRNAs, we searched for protein coding genes in adjacent regions of the lncRNA sequence. The correlation between lncRNAs and coding genes was calculated to predict trans-acting lncRNA target genes.

# Enrichment analyses and construction of the protein-protein interaction network

GO annotation and KEGG pathway enrichment analysis were performed for differentially expressed genes and lncRNA target genes to explore the main biological functions of the differentially expressed mRNA and lncRNAs. The statistical enrichment of differentially expressed genes was analyzed using DAVID 6.8. The STRING website was used to construct a protein-protein interaction network, and the Cytoscape software was used to visualize it.

# Quantitative real-time RT-PCR

Gene and lncRNA specific primers were designed using the Primer-BLAST tool, and the amplification efficiency of primers was confirmed by general PCR (Supplementary Table 2). Approximately 0.5 μg of each RNA sample was used to synthesize cDNA templates using the HiFiScript gDNA Removal cDNA kit (CWbiotech, China). A QuantStudio3 Real-time PCR Instrument (Thermo Fisher Scientific, USA) was used for the qRT-PCR assay, and the reaction system was set up according to the manufacturer's instructions of the 2×Plus SYBR real-time PCR kit (CWbiotech). The temperature program encompassed an initial denaturation step at 94 °C for 3 min, followed by 40 cycles of 95 °C for 15s, 60 °C for 15s, and 72℃ for 30s. The housekeeping gene β-actin was used as the control for normalization, and the experiments were performed in triplicate. The $2^{-\Delta\Delta CT}$ method was used to calculate the relative gene expression levels.

# Western blot analysis

RIPA buffer (Beyotime, Shanghai, China) supplemented with protease inhibitor (Pierce, Bradenton, Florida, USA) was used to extract the total proteins. The lysates were centrifuged at 1,2000 rpm for 10 min, and the supernatant was boiled in sodium dodecyl sulfate (SDS) loading buffer (Beyotime, Shanghai, China). After separation on a 12% acrylamide SDS-PAGE gel, the protein bands were transferred onto a PVDF membrane (Millipore, Massachusetts, USA). The membrane was incubated with different primary antibodies, against p38, p-p38, pERK1/2 and p-pERK1/2, respectively, which were purchased from cell signal Technology. A Bio-Rad ChemiDoc XRS+ image analyzer system was used to photograph the blots.

# Statistical analysis

All data were presented as the means ±standard error (SE), and the statistical analysis of the qRT-PCR assay was implemented using GraphPad Prism 8. The statistical significance of differences between Jiaxing Black and Large White pigs was assessed using Student's *t*-test, with $P < 0.05$ as the threshold.

# Abbreviations

SC: subcutaneous; IM: intramuscular; lncRNAs: long noncoding RNAs; JX pig: Jiaxing Black pig; LW pig: Large White pig; DEGs: differentially expressed genes; DELs: differentially expressed lncRNAs; GO: Gene Ontology; KEGG: Kyoto Encyclopedia of Genes and Genomes; MCC: Maximal Clique Centrality; MMPs: matrix metalloproteases.

# Declarations

### Ethics approval and consent to participate

Jiaxing University Animal Care Committee provided official ethics board approval for this study. Tissues used in this study were collected from pigs maintained and used according to the approved protocols.

### Consent for publication

Not applicable.

### Availability of data and materials

The data sets supporting the results of this article are included within the manuscript and its additional files. The raw datasets generated during the current study are not publicly available due as analysis is still ongoing, but are available from the corresponding author on reasonable request.

### Competing interests

The authors declare that they have no competing interests.


### Funding

This work was supported by Zhejiang Natural Science Foundation (LY20C170003), Initial Scientific Research Fund of Young Teachers in Jiaxing University (No.70518061) and General Research Project of Zhejiang Provincial Department of Education (No. Y201942267).


### Authors' contributions

DZ designed the experiments and wrote the paper, and provided the experimental funding. WW designed the experiments and performed cell culture. DZ, XH, CZ and KX performed, analyzed and interpreted the study. JZ designed the study, revised the paper, and provided the experimental funding. All authors analyzed the results and approved the final version of the manuscript.


### Acknowledgements

The authors are grateful to Zhejiang Qinglian Food Co., Ltd., Jiaxing Dayunhe Ecological Animal Husbandry Co., Ltd and Zhejiang Huatong meat products Co., Ltd. for providing experimental animals.


## References


1. Wu W, Zhang D, Yin Y, Ji M, Xu K, Huang X, Peng Y, Zhang J. Comprehensive transcriptomic view of the role of the LGALS12 gene in porcine subcutaneous and intramuscular adipocytes. BMC Genom. 2019;20(1):509.
2. Li M, Zhu L, Li X, Shuai S, Teng X, Xiao H, Li Q, Chen L, Guo Y, Wang J. Expression profiling analysis for genes related to meat quality and carcass traits during postnatal development of backfat in two pig breeds. Sci China C Life Sci. 2008;51(8):718–33.
3. Newcom D, Baas T, Schwab C, Stalder K. Genetic and phenotypic relationships between individual subcutaneous backfat layers and percentage of longissimus intramuscular fat in Duroc swine. J Anim Sci. 2005;83(2):316–23.

4. Cui J, Zeng Y, Wang H, Chen W, Du J, Chen Q, Hu Y, Yang L. The effects of DGAT1 and DGAT2 mRNA expression on fat deposition in fatty and lean breeds of pig. Livest Sci. 2011;140(1–3):292–6.
5. Yuan Z, Song D, Wang Y. The novel gene pFAM134B positively regulates fat deposition in the subcutaneous fat of Sus scrofa. Biochem Biophys Res Commun. 2014;454(4):554–9.
6. Yan WJ, Li XM, Jiang YX. **Fatty Acids in Intramuscular and Subcutaneous Fat of Jinhua Ham [J]**. *Food and Fermentation Industries* 2005, 2.
7. Liu X, Liu K, Shan B, Wei S, Li D, Han H, Wei W, Chen J, Liu H, Zhang L. A genome-wide landscape of mRNAs, lncRNAs, and circRNAs during subcutaneous adipogenesis in pigs. J Anim Sci Biotechnol. 2018;9:76.
8. Miao Z, Wang S, Zhang J, Wei P, Guo L, Liu D, Wang Y, Shi M. Identification and comparison of long non-conding RNA in Jinhua and Landrace pigs. Biochem Biophys Res Commun. 2018;506(3):765–71.
9. Zhang B: **China National Commission of Animal Genetic Resources**. *Animal genetic resources in China: Horses, Donkeys, Camels China Agricultural Press, China* 2011.
10. Chen H, Huang M, Yang B, Wu Z, Deng Z, Hou Y, Ren J, Huang L. Introgression of Eastern Chinese and Southern Chinese haplotypes contributes to the improvement of fertility and immunity in European modern pigs. Gigascience. 2020;9(3):giaa014.
11. Huang W, Zhang X, Li A, Xie L, Miao X. Genome-wide analysis of mRNAs and lncRNAs of intramuscular fat related to lipid metabolism in two pig breeds. Cell Physiol Biochem. 2018;50(6):2406–22.
12. Crujeiras A, Díaz-Lagares A, Carreira M, Amil M, Casanueva F. Oxidative stress associated to dysfunctional adipose tissue: a potential link between obesity, type 2 diabetes mellitus and breast cancer. Free Radic Res. 2013;47(4):243–56.
13. Medina-Remón A, Kirwan R, Lamuela-Raventós RM, Estruch R. Dietary patterns and the risk of obesity, type 2 diabetes mellitus, cardiovascular diseases, asthma, and neurodegenerative diseases. Crit Rev Food Sci Nutr. 2018;58(2):262–96.
14. Kuzmuk KN, Schook LB. Pigs as a model for biomedical sciences. The genetics of the pig. 2011;2:426–44.
15. Gün G, Kues WA. Current progress of genetically engineered pig models for biomedical research. Biores Open Access. 2014;3(6):255–64.
16. Zhang GH, Lu JX, Chen Y, Zhao YQ, Guo PH, Yang JT, Zang RX. Comparison of the adipogenesis in intramuscular and subcutaneous adipocytes from Bamei and Landrace pigs. Biochem Cell Biol. 2014;92(4):259–67.
17. Hou X, Yang Y, Zhu S, Hua C, Zhou R, Mu Y, Tang Z, Li K. Comparison of skeletal muscle miRNA and mRNA profiles among three pig breeds. Mol Genet Genomics. 2016;291(2):559–73.
18. de Almeida AM, Bendixen E. Pig proteomics: a review of a species in the crossroad between biomedical and food sciences. J Proteomics. 2012;75(14):4296–314.

19. Murgiano L, D'Alessandro A, Egidi MG, Crisa A, Prosperini G, Timperio AM, Valentini A, Zolla L. Proteomics and transcriptomics investigation on longissimus muscles in Large White and Casertana pig breeds. J Proteome Res. 2010;9(12):6450–66.
20. Kumar H, Srikanth K, Park W, Lee S-H, Choi B-H, Kim H, Kim Y-M, Cho E-S, Kim JH, Lee JH. Transcriptome analysis to identify long non coding RNA (lncRNA) and characterize their functional role in back fat tissue of pig. Gene. 2019;703:71–82.
21. Gao P, Guo X, Du M, Cao G, Yang Q, Pu Z, Wang Z, Zhang Q, Li M, Jin Y. LncRNA profiling of skeletal muscles in Large White pigs and Mashen pigs during development. J Anim Sci. 2017;95(10):4239–50.
22. Schmitz SU, Grote P, Herrmann BG. Mechanisms of long noncoding RNA function in development and disease. Cell Mol Life Sci. 2016;73(13):2491–509.
23. van Solingen C, Scacalossi KR, Moore KJ. Long noncoding RNAs in lipid metabolism. Curr Opin Lipidol. 2018;29(3):224.
24. Zhang W, Song Qq, Wu F, Zhang Jz Xu, Ms L, Hh H, Zj. Gao Hx, Xu Ny: **Evaluation of the four breeds in synthetic line of Jiaxing Black Pigs and Berkshire for meat quality traits, carcass characteristics, and flavor substances**. Anim Sci J. 2019;90(4):574–82.
25. Cohen P, Levy JD, Zhang Y, Frontini A, Kolodin DP, Svensson KJ, Lo JC, Zeng X, Ye L, Khandekar MJ. Ablation of PRDM16 and beige adipose causes metabolic dysfunction and a subcutaneous to visceral fat switch. Cell. 2014;156(1–2):304–16.
26. Poulos SP, Hausman DB, Hausman GJ. The development and endocrine functions of adipose tissue. Mol Cell Endocrinol. 2010;323(1):20–34.
27. He Y, Zhang H, Teng J, Huang L, Li Y, Sun C. Involvement of calcium-sensing receptor in inhibition of lipolysis through intracellular cAMP and calcium pathways in human adipocytes. Biochem Biophys Res Commun. 2011;404(1):393–9.
28. Xue B, Greenberg AG, Kraemer FB, Zemel MB. Mechanism of intracellular calcium ([Ca2+] i) inhibition of lipolysis in human adipocytes. FASEB J. 2001;15(13):2527–9.
29. Li H, Marshall AJ. Phosphatidylinositol (3, 4) bisphosphate-specific phosphatases and effector proteins: a distinct branch of PI3K signaling. Cell Signal. 2015;27(9):1789–98.
30. Manning BD, Tee AR, Logsdon MN, Blenis J, Cantley LC. Identification of the tuberous sclerosis complex-2 tumor suppressor gene product tuberin as a target of the phosphoinositide 3-kinase/akt pathway. Mol Cell. 2002;10(1):151–62.
31. Plum L, Rother E, Münzberg H, Wunderlich FT, Morgan DA, Hampel B, Shanabrough M, Janoschek R, Könner AC, Alber J. Enhanced leptin-stimulated Pi3k activation in the CNS promotes white adipose tissue transdifferentiation. Cell Metab. 2007;6(6):431–45.
32. Sharma BR, Kim HJ, Rhyu DY. Caulerpa lentillifera extract ameliorates insulin resistance and regulates glucose metabolism in C57BL/KsJ-db/db mice via PI3K/AKT signaling pathway in myocytes. J Transl Med. 2015;13(1):62.

33. Sun Y, Liu W-Z, Liu T, Feng X, Yang N, Zhou H-F. Signaling pathway of MAPK/ERK in cell proliferation, differentiation, migration, senescence and apoptosis. J Recept Signal Transduct Res. 2015;35(6):600–4.
34. Capolongo G, Suzumoto Y, D'Acierno M, Simeoni M, Capasso G, Zacchia M. ERK1, 2 Signalling Pathway along the Nephron and Its Role in Acid-base and Electrolytes Balance. Int J Mol Sci. 2019;20(17):4153.
35. Bost F, Aouadi M, Caron L, Binétruy B. The role of MAPKs in adipocyte differentiation and obesity. Biochimie. 2005;87(1):51–6.
36. Cao D, Ma F, Ouyang S, Liu Z, Li Y, Wu J. Effects of macrophages and CXCR2 on adipogenic differentiation of bone marrow mesenchymal stem cells. J CELL PHYSIOL. 2019;234(6):9475–85.
37. Deng W, Chen H, Su H, Wu X, Xie Z, Wu Y, Shen H. **IL6 Receptor Facilitates Adipogenesis Differentiation of Human Mesenchymal Stem Cells through Activating P38 Pathway**. *Int J Stem Cells* 2019.
38. Zhang S, Cao H, Li Y, Jing Y, Liu S, Ye C, Wang H, Yu S, Peng C, Hui L, et al. Metabolic benefits of inhibition of p38alpha in white adipose tissue in obesity. PLoS Biol. 2018;16(5):e2004225.
39. Lolmède K, Duffaut C, Zakaroff-Girard A, Bouloumié A. Immune cells in adipose tissue: key players in metabolic disorders. Diabetes Metab. 2011;37(4):283–90.
40. Mraz M, Haluzik M. The role of adipose tissue immune cells in obesity and low-grade inflammation. J Endocrinol. 2014;222(3):R113–27.
41. Majdoubi A, Kishta OA, Thibodeau J. Role of antigen presentation in the production of pro-inflammatory cytokines in obese adipose tissue. Cytokine. 2016;82:112–21.
42. Guzik TJ, Skiba DS, Touyz RM, Harrison DG. The role of infiltrating immune cells in dysfunctional adipose tissue. Cardiovasc Res. 2017;113(9):1009–23.
43. Lumeng CN. Innate immune activation in obesity. Mol Aspects Med. 2013;34(1):12–29.
44. Joffe YT, Collins M, Goedecke JH. The relationship between dietary fatty acids and inflammatory genes on the obese phenotype and serum lipids. Nutrients. 2013;5(5):1672–705.
45. Van Hul M, Lijnen HR. Matrix metalloproteinase inhibition impairs murine adipose tissue development independently of leptin. Endocr J. 2011;58(2):101–7.

# Figures

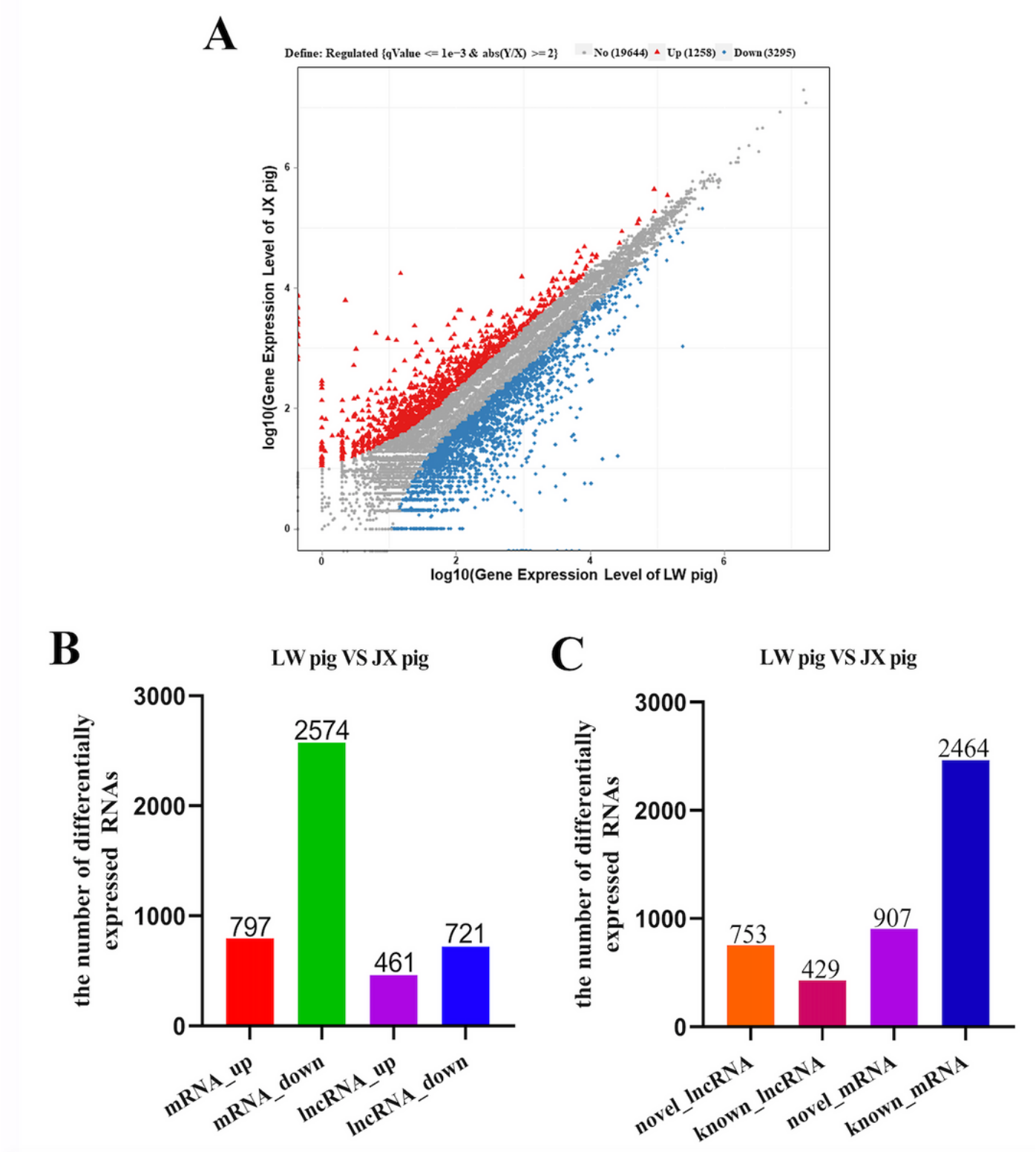


## Figure 1

Differentially expression characteristics of coding genes and lncRNAs between LW and JX pigs. A. The volcano plot of differentially expressed transcripts, including mRNAs and lncRNAs. B. The number of up-regulated and down-regulated transcripts in differentiated subcutaneous adipocyte. C. The distribution of transcript number of mRNA and lncRNAs identified in two pig breeds.

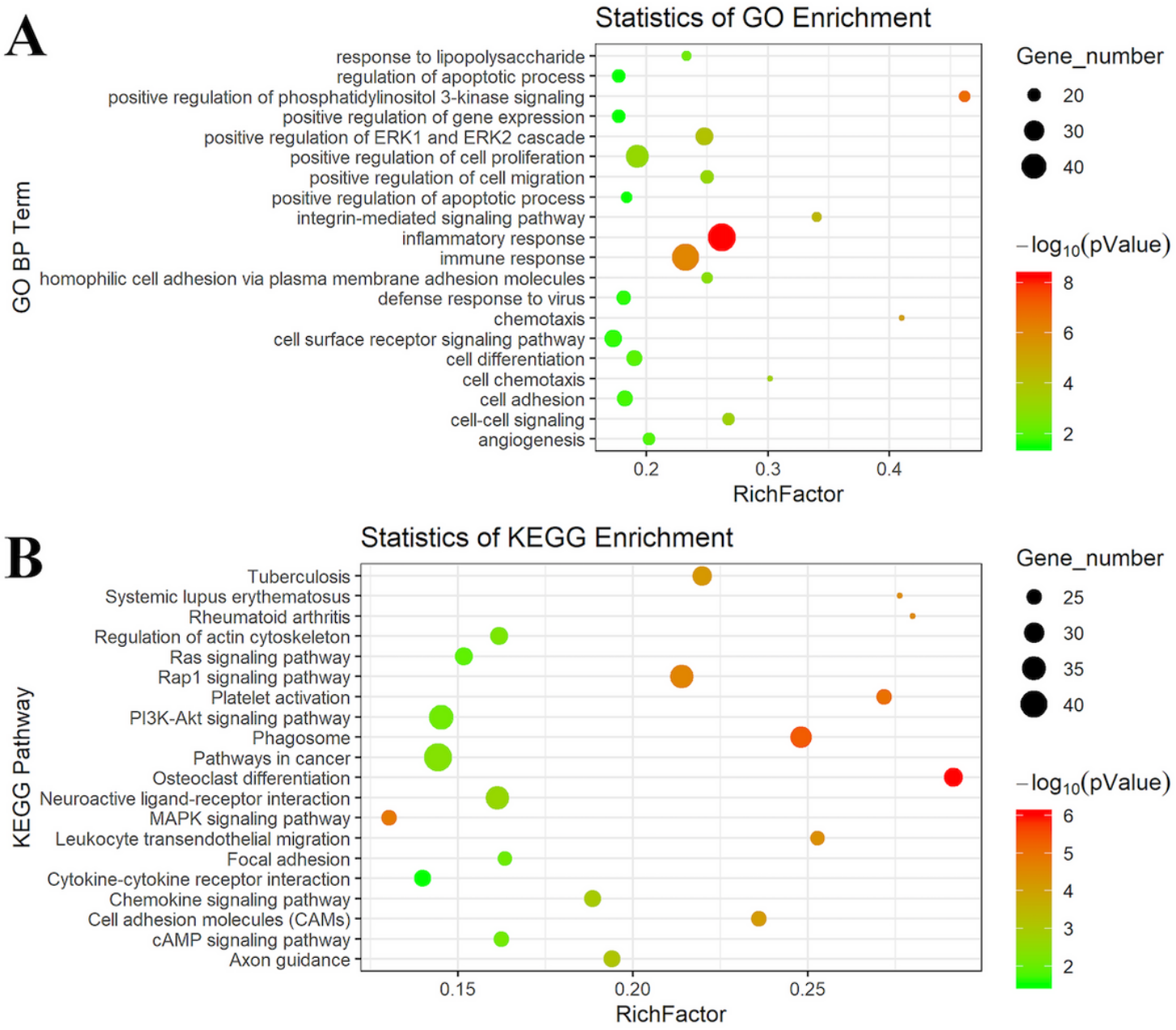


## Figure 2

GO annotation and KEGG pathway analysis of DEGs. A. Go terms distribution of DEGs under biological processes. B. Enrichment of DEGs in signaling pathways. Each bubble represents a term. The size of the bubble indicates the number of involved genes. The colors indicate P values, and the significance level of enrichment was set at P value < 0.05, and enrichment terms was ranked by DEGs number.

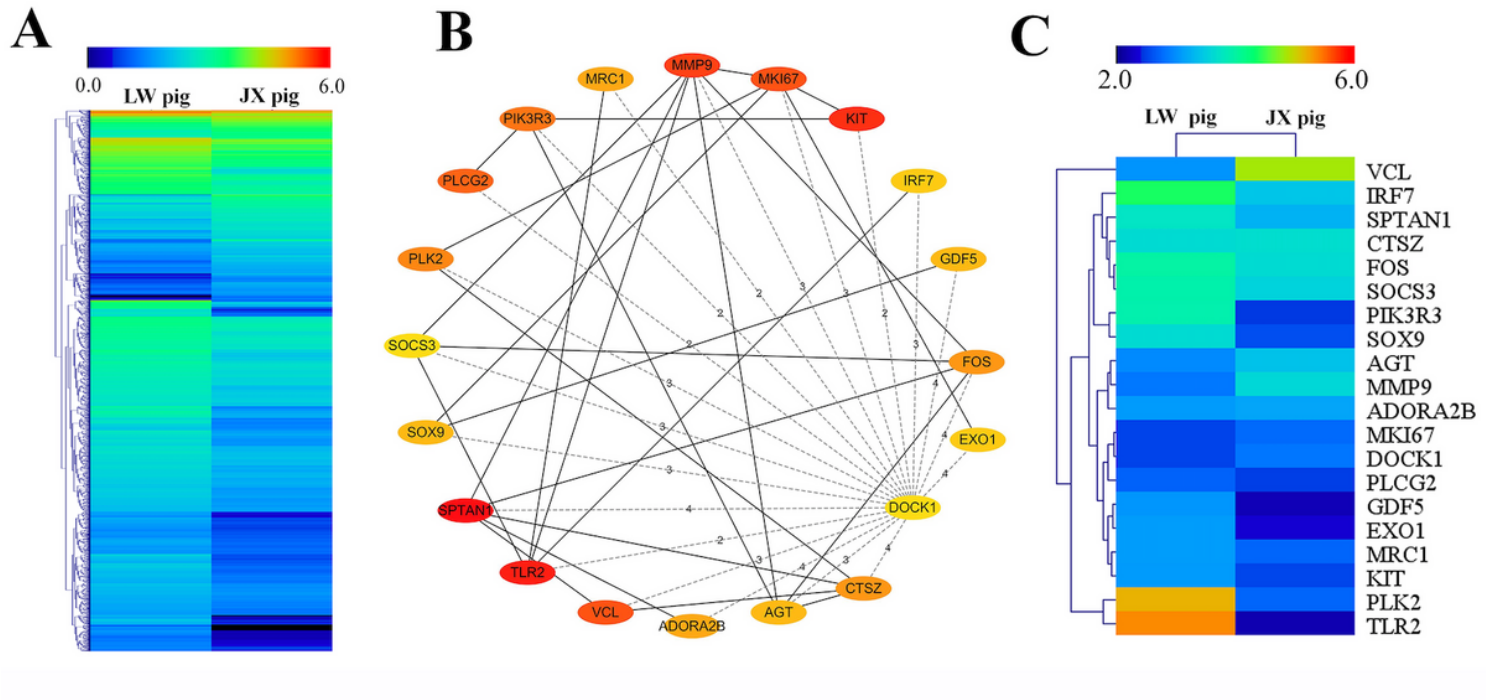


## Figure 3

Protein-protein interaction (PPI) network analysis by cytoscape of DEGs. A. Unsupervised hierarchical clustering of the expression profile of significant genes of DEGs. B. The PPI network of DEGs according to MCODE. C. Unsupervised hierarchical clustering of the expression profile of hub genes in PPI network.

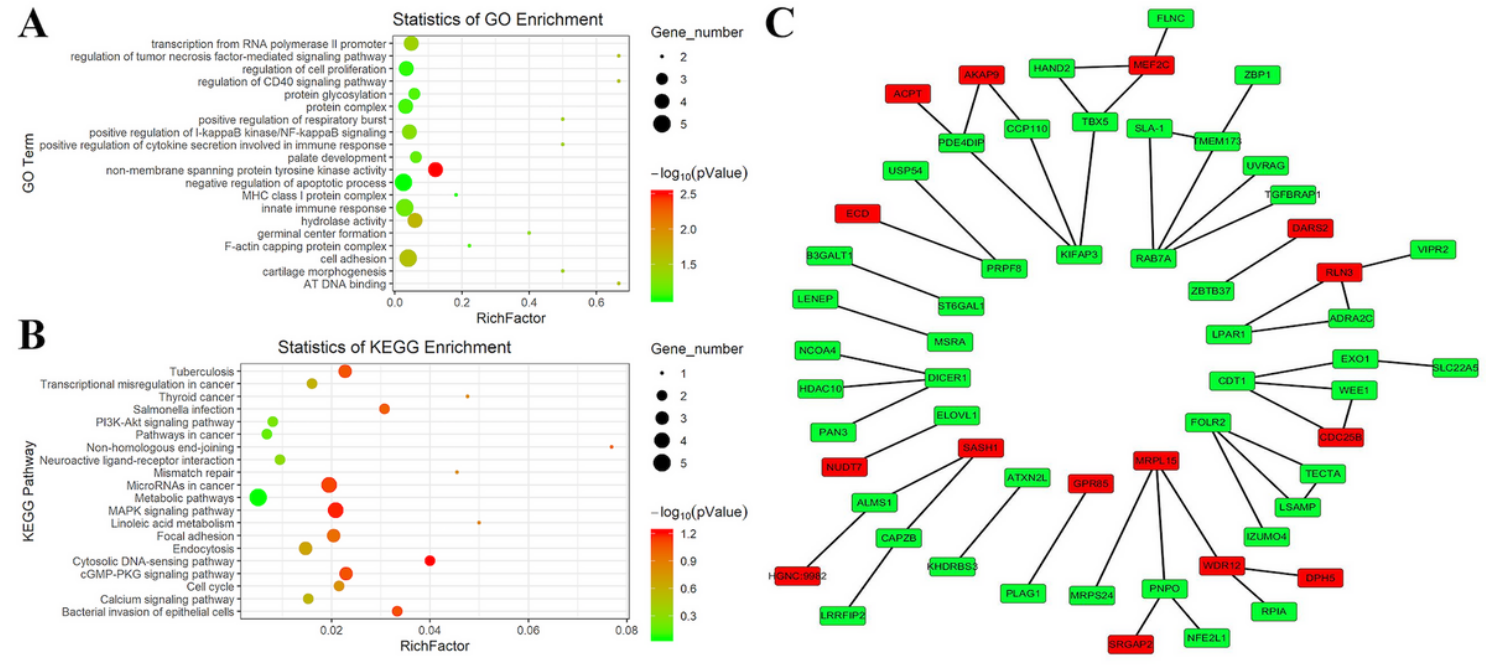


## Figure 4

Functional enrichment and PPI network analysis of DELs-target genes. GO enrichment (A) and KEGG pathway enrichment (B) of the target genes. C. PPI network of DELs-target genes, red means upregulated

genes and green means downregulated genes.

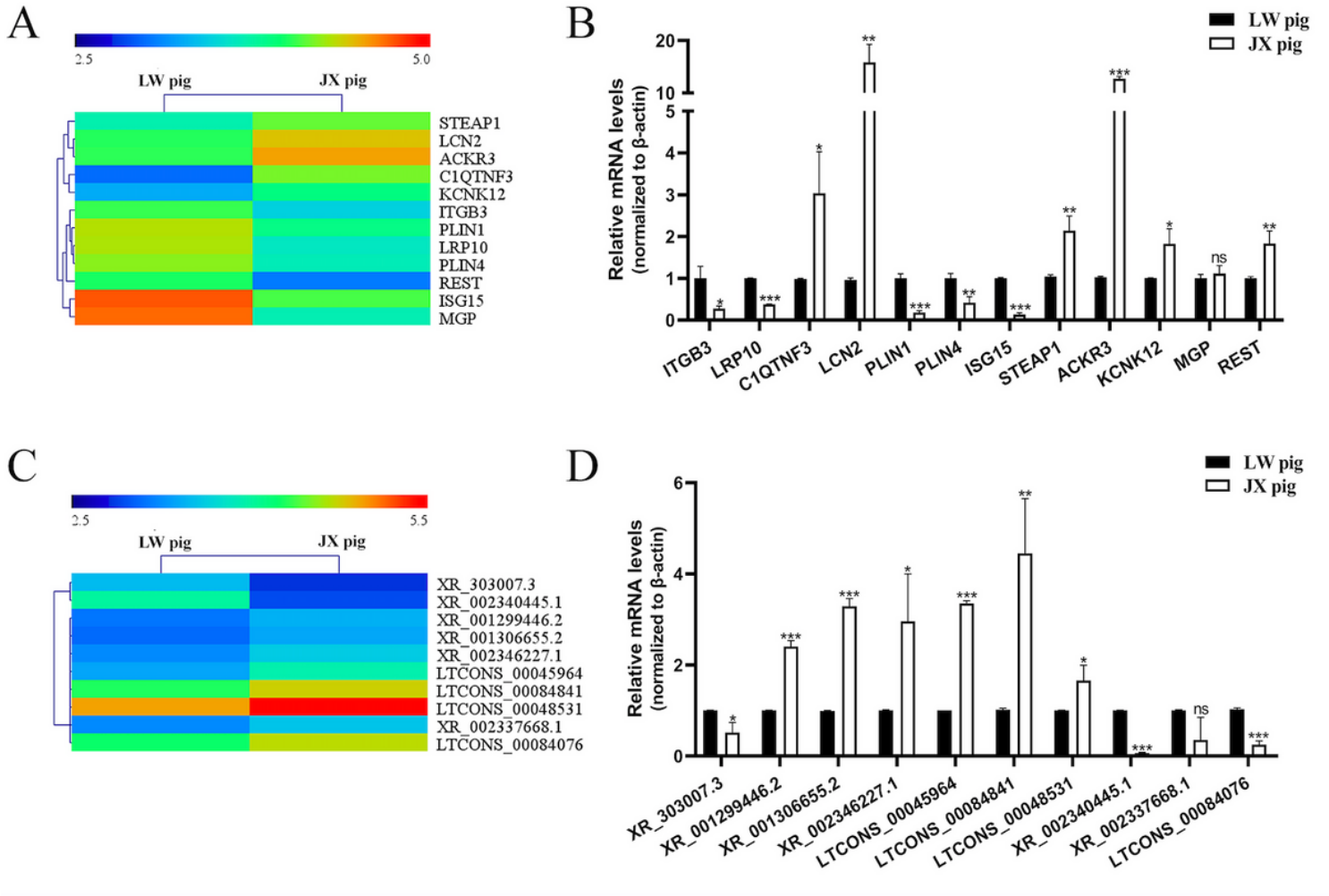


## Figure 5

Q-PCR validation of DEGs and DELs in differentiated subcutaneous adipocyte between LW and JX pigs. A. Unsupervised hierarchical clustering of the expression profile of twelve randomly selected DEGs. B. Q-PCR validation of the expression level of twelve randomly selected DEGs. C. Unsupervised hierarchical clustering of the expression profile of ten randomly selected DELs. D. Q-PCR validation of the expression level of ten randomly selected DELs. *: P<0.05; **: P<0.01; ***: P<0.001.

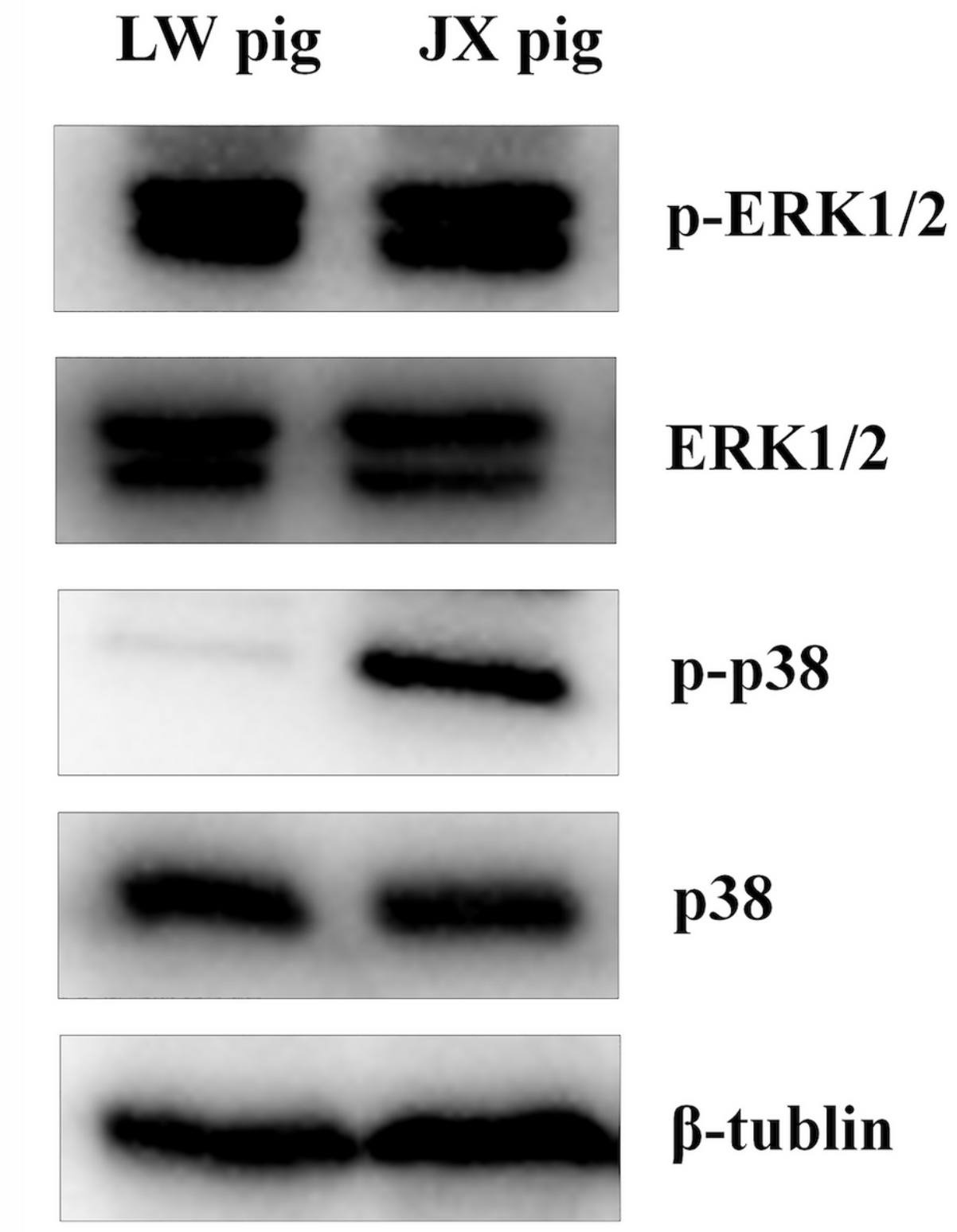


**Figure 6**

Verification of MAPK signaling pathway by western blot. The total protein abundance and phosphorylated level of p38 and ERK1/2 were observed in subcutaneous fat tissue of LW and JX pigs, and the protein level of β-tublin was used as a control.

## Supplementary Files

This is a list of supplementary files associated with this preprint. Click to download.

- Additionalfile1.pdf